IAS Diagnosis based on a BEAring Frequency estimation Method (BeaFEM)

R. Bertoni [1], **H. André** [2]
[1] Vibratec
28 chemin du petit bois, 69130 Ecully, France
e-mail: **renaud.bertoni@vibratec.fr**
[2] Université de Lyon, Université Jean Monnet, LASPI EA3059,
42023 Saint-Etienne, France
20 Avenue de Paris, 42334 Roanne Cedex, France
e-mail: **h.andre@univ-st-etienne.fr**

Abstract
Early detection of bearing faults is one of the major industrial concerns, brought to the forefront by miniaturization and the increase in component rotation speeds. Many post-processing methodologies based on different types of sensors have been proposed in the past, without any of them really distinguishing themselves from the classical method of squared envelope analysis on an accelerometric signal.
This paper presents an original diagnostic method which, associated with the analysis of the Instantaneous Angular Speed (IAS) signal, brings a new contribution to the subject. This method is based on the estimation of the characteristic frequency, optimized to detect and track a bearing fault. If the characteristic frequencies BPFO, BPFI and FTF are unknown a priori because they depend on poorly controlled parameters (such as the contact angle), they remain kinematically linked by the cage motion.
The results obtained on an industrial test bench show that it is possible to detect the generation of an inner ring defect with an incremental encoder In this paper, the BEAring Frequency Estimation Method (BeaFEM) is presented and tested on two application cases: an inner ring fault and a ball fault. The ball defect is particularly detailed because the detection of its characteristic frequency is more difficult. Indeed, when it leaves the loading zone, the ball undergoes a slip independent of the cage motion and the characteristic frequency of the ball defect (BSF) is slightly lower than the one obtained by optimizing the BPFO-BPFI-FTF characteristic frequencies via BeaFEM. This diffuclty is circumvented by applying the enveloppe on the IAS signal.
This paper therefore presents an original processing method to diagnose several types of bearing defects. Experimentally validated on a fatigue campaign, the method combined with the measurement of IAS appears as a new and very promising prognostic tool.

1 Introduction

Bearing monitoring is a major concern for industry since nearly one century, and still the topic of many scientific researches as no simple, efficient method exists to detect and track faults. The most widespread technique used is vibration monitoring, with different variation generally based on envelope analysis [1] [2]. Nowadays, these techniques are complemented by the angular domain observation of the signals, particularly adapted to analyze the cyclostationary properties of rotating machine [3, 4]. As much as the term vibration monitoring echoes accelerometry, the angular domain appeals to any physical signal synchronously sampled with the angle of a shaft of the rotating machine. Among the signals classically analyzed in the angular domain, the analysis of instantaneous angular speed (IAS), obtained by Elapsed Time (ET), has the advantage of providing a signal intrinsically sampled with the shaft where the encoder is installed. Indeed, the IAS observation allows to separate sharply the deterministic components such as gear mesh frequencies or shaft rotation frequency, letting the phenomena of interest only on a few frequency channels. Consequently, IAS

based diagnosis mostly rely on a simple discrete Fourier transform.

In a recent past, several researches have demonstrated the ability of IAS analysis to be a powerful bearing fault detection tool. Among them, Remmond et al have shown the interest of using an incremental encoder for rotating machine diagnosis [5]; Renaudin et al used an encoder directly fitted on the monitored bearing [6], and André et al have shown afterward that it is possible to detect a bearing fault on a wind turbine shaft by the use of an encoder installed further on the shaft line [7]. This last point is a real advantage compared to the accelerometry, which requires generally a sensor per bearing to monitor.

Another underestimated advantage of IAS monitoring is its intrinsic angular nature. Indeed, as instantaneous speed signals are naturally angularly sampled, they offer an almost perfect synchronisation with cyclic phenomena. If the practice in bearing vibration diagnosis is to consider CS2 faults because of the hazard attributed to cage slip, the practice in IAS diagnosis is to consider it CS1. This assumption, which may be provocative for the specialists of accelerometric monitoring, will be discussed in this paper.

The work included in this paper assumes that the signature of a defective bearing is deterministic, and of constant angle frequency during a measurement performed under stationary conditions. An approach to monitor a bearing defect whose characteristic frequency evolves with the defect degradation is proposed. The method is based on the scan of possible bearing contact angles, and associates the evolution of the characteristic frequency with the progressive evolution of the fault. In a first section, some reminders about the bearings faults are provided. Then, a robust method for the detection of bearing defects is depicted: the BEAring Frequency Estimation Method. A particular care is taken to explain the specific behaviour of the ball fault. The proposed technique is validated experimentally during an endurance test on a helicopter transmission kinematic chain, whose results are provided in section 4. Finally, a discussion regarding the method application and its perspectives is proposed.

2 Bearing faults description and the kinematic link between them

Due to their essential nature for any motion transmission, bearings are widely documented in the literature, whether it be on the thermal, lubrication or mechanical aspects. In the latter case, the focus is on the vibration signature associated with the generation of a fault. The four main types of bearing fault are inner ring fault, outer ring fault, cage fault and ball fault. It should be noted that the term "bearing fault" traditionally refers to the particular case of a fault located on one of the components of the bearing, and therefore corresponds to a particular vibration signature. These signatures, well known in the literature, are characterised by their (cyclo)periodicity whose frequencies are described in the table 1 .

Thoses characteristic frequencies depend on the bearing geometric characteristics: number of balls n, ball diameter d, raceway diameter D, contact angle α. The latter is expected to be linked with several parameters: the ratio between axial and radial loading (for deep groove roller bearing) along with the deformation of the loaded bearing, the mounting conditions, thermal expansion of the bearing, etc. Furthermore, these characteristic frequencies result from the kinematic relations associated with the hypothesis of a slip-free rolling between the rings and the rolling elements. All the rolling elements are considered homokinetic, the cage is considered non-deformable, the relative position of the shaft to the bore is static.

In practice, an uncertainty of a few percent exists on the characteristic frequencies, usually mitigated by the fact that accelerometers are placed close to the monitored bearing, and that the emergence of a peak in a frequency range close to the theoretical one is attributed to the fault. In the present paper, a global method for supervising the bearing is proposed, based on the coherence between the characteristic frequencies: the BEAring Frequency Estimation Method. The main hypothesis of this method is that it is inconsistent to identify characteristic frequencies that do not correspond to the same combination of geometrical parameters (n, d, D and α). Indeed, as can be seen in the table 1, the equations are linked to the same parameter α

through a trigonometric function.

Table 1: rolling element characteristic frequencies

fault type	analytical formula
Outer race (BPFO)	$n/2 \cdot f_r(1 - d/D \cdot cos\alpha)$
Inner race (BPFI)	$n/2 \cdot f_r(1 + d/D \cdot cos\alpha)$
Cage (FTF)	$f_r/2(1 - d/D \cdot cos\alpha)$
Ball (BSF)	$f_r \cdot D/2d(1 - (d/D \cdot cos\alpha)^2)$

3 The bearing frequency estimation method : BeaFEM

3.1 General concept

An important aspect of the method proposed by Antoni et al. to design condition indicators [8] is that an indicator is related to the comparison of two statistical hypotheses and optimal only in this perspective. In the case of a faulty bearing, the optimal indicator will be the one involving the stationnary property of a healthy bearing signal to the cyclostationarity of a faulty one. It can be be approximated by the sum of the spectral components of the IAS amplitude spectrum. The bearing health can be practically assessed by calculating $I(\alpha)$, sum of several spectral components whose frequency exactly corresponds to the characteristic frequency of the bearing. For a given geometry,this frequency depends theoretically mostly on the contact angle α. The values that $I(\alpha)$ would take for all possible values of contact angle α are therefore calculated.

Let $\mathcal{A}$ be the interval scrutinized for α; $I(\alpha)$ is then defined such as:

$$\forall \alpha \in \mathcal{A}, I(\alpha) = \sum_{h=1..H} \sum_{m=-M..M} \xi_i \cdot |X(hf_i(\alpha)+mf_1)| + \xi_o \cdot |X(hf_o(\alpha)+mf_1)| + \xi_c \cdot |X(hf_c(\alpha)+mf_1)| \tag{1}$$

with

- X an estimator of the IAS signal PSD;
- $f_i(\alpha)$, $f_o(\alpha)$, $f_c(\alpha)$ the inner ring fault, outer ring fault, cage fault characteristic frequency, as a function of the angle α ;
- f_1 the rotation frequency of the defective bearing's shaft;
- ξ_i, ξ_o and ξ_c binary interrupters used either to consider or neglect inner ring fault, outer ring fault and cage fault characteristic frequencies respectively;
- m the number of side-bands includes in the calculation, and h the number of harmonics

The equation (1) can be modeled to scan indifferently inner ring faults, outer rings faults or cage faults (BPFI, BPFO, FTF) either alone or combined. Only the ball defect cannot be searched using this method. Indeed, although the slip-free condition is acceptable for rings and cages once the bearing is loaded, it is much more difficult to respect for rolling elements that are not loaded. As soon as the load is radial, its uneven distribution will limit the slip-free condition fulfilment to the few loaded rolling elements. in other words, the ball defect does not have a CS1 character. As a result, the BeaFEM approach outlined in the following concerns only inner and outer ring and cage failures, and may not be satisfactory for Ball faults.

A possible solution to this bias would be to adopt a CS2 approach: X would then be an estimate of the squared envelope spectrum, as it would be in the case of vibration measurements.

3.2 BeaFEM indicators

Let $I(\alpha)$ be a scalar whose value depends on α; BeaFEM indicator is the pair (I_{opt}, α_{opt}) defined such as:

$$\begin{aligned} I_{opt} &= \max_{\alpha} I(\alpha) \\ \alpha_{opt} &= \operatorname*{argmax}_{\alpha} I(\alpha) \end{aligned} \tag{2}$$

The indicator I_{opt} is the maximized summed amplitude of the scrutinized bearing characteristic frequencies. α_{opt} is the contact angle corresponding to this maximized value.
The joint observation of these two scalars allows to search the presence of a defect, and to evaluate the detection robustness. By combining only the frequency components that correspond to the same value of the parameter α, I_{opt} evaluates the severity of the fault. Additionaly, the distribution of α_{opt} determnine the presence of the defect. The regularity of the estimate as well as the observation of a slow and continuous trend can confirm the evolution of a defect by underlining its impact on the parameter of the characteristic frequency.

In other words, I_{opt} is an image of the severity of the defect while α_{opt} allows to test the reliability of the estimation.

The experimental validation of BeaFEM is the topic of the next chapter.

4 Experimental validation

4.1 Test bench presentation

During the collaborative project MACCHELI (MAintenance de Chaîne Cinématique d'HELIcoptère), a test bench representative of a helicopter kinematic chain portion was built. It is composed of four shafts and three gear stages, with a global reduction ratio of 4.6. (figure 1).

The low speed shaft is speed controlled, while a resistive torque is applied to the high speed shaft. In order to approach the real operational conditions, inertias are added on the shafts. Lubrication (oil type, distribution and temperature) as well as mounting parameters (clearances, bearings) are equivalent to those of the real motor. The main differences between the test bench and the complete powertrain are the rotation speed (10 times lower) and the absence of background noise related to the engine combustion.

The project aims at monitoring faults on the high speed shaft roller bearings (figure 1). Both bearings are strictly identical: same manufacturer and dimensions. The DE bearing is axially preloaded using wave washers so as to increase the defect generation for the endurance tests.

In terms of instrumentation, speed sensors are positioned on each shaft (sensors C1 o C4). In addition, a B&K 4525 accelerometer is glued on each bearing housing (sensors a1 and a2). In this paper, only the speed sensor C4 is considered. Mounted on the shaft carrying the faulty bearings, this incremental encoders Kuebler 5821 has a resolution of 2048 points per revolution.

The acquisitions are carried out using a LMS TestLab system. The "elapsed time" method described in [9] is used to acquire the signals via an 820 MHz tacho card. Each measurement lasts 60 seconds.

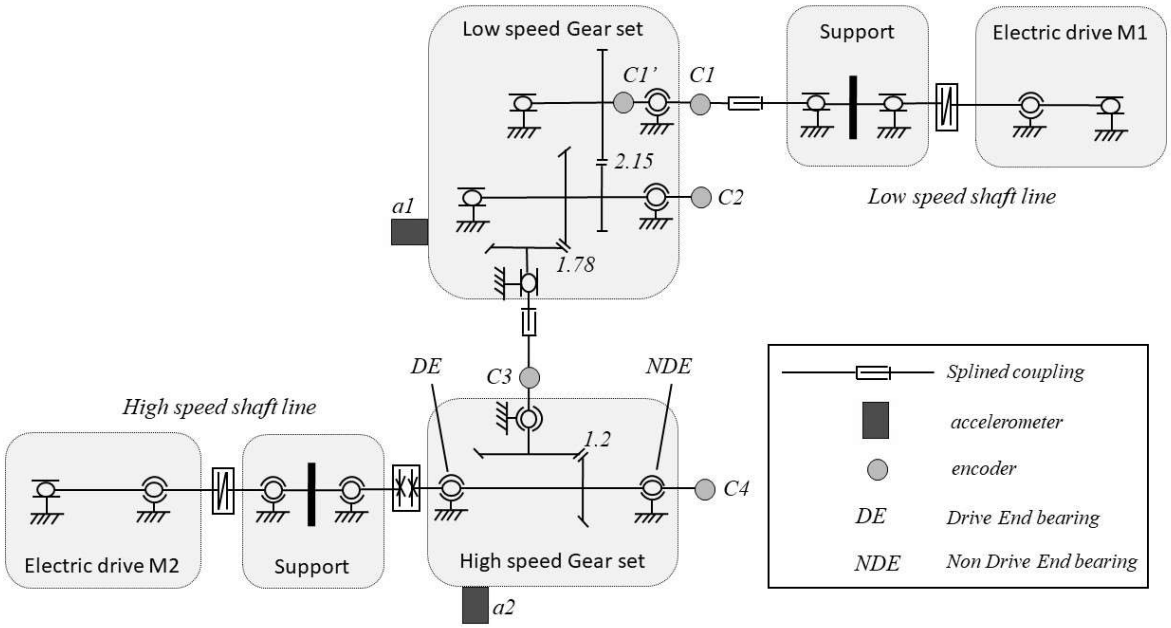

Figure 1: test bench kinematics

4.2 Tests performed

Two endurance campaigns were led on the test bench: one with a seeded fault on the DE bearing, and one without any initial fault. The second test campaign is presented here. This measurement campaign was conducted with a healthy DE bearing and the NDE bearing used during the first campaign. As the latter was not inspected between the two measurement campaigns, no information about its wear is available at the beginning of the endurance is availalbe. The hypothesis is made that it is healthy at this point.

The axial preload to which the DE bearing is subjected is increased by the addition of wave washers: this modification wears more quickly the bearings than the normal life conditions. Due to the mounting, both bearings had an equiprobability of failure. Note that the ratio F_{axial}/F_{radial} has not been modified during the endurance and is considered constant. The test lasted 75 hours.

At the end of the endurance test, two defects were visible on the DE and NDE bearing inner rings (figure 2), while five balls of the DE bearing were damaged (figure 3). These defects are investigated in the rest of the paper.

4.3 Inner ring fault search

BeaFEM is applied to the IAS signals measured during endurance testing, with the aim of identifying the presence of a potential bearing defect. Prior to this, the deterministic phenomena such as the shaft and gear mesh frequencies were removed. Indeed, these components carry a lot of energy although they are not related to the phenomenon of interest. Among the most commonly used cleaning methods are those based on linear prediction filtering [10], Cepstrum prewhitening [11] or even time synchronous average [12]. This cleaning is performed by substracting the Rotation Domain Averaging (RDA), trivial extension of the Time Synchronous Averaging (TSA) to the cyclic case. RDA is defined for a continuous signal $x(\theta)$ described in the angular domain such as:

$$y_s(\theta) = 1/N \sum_{r=0}^{N} x(\theta + r \cdot \Theta_s) \tag{3}$$

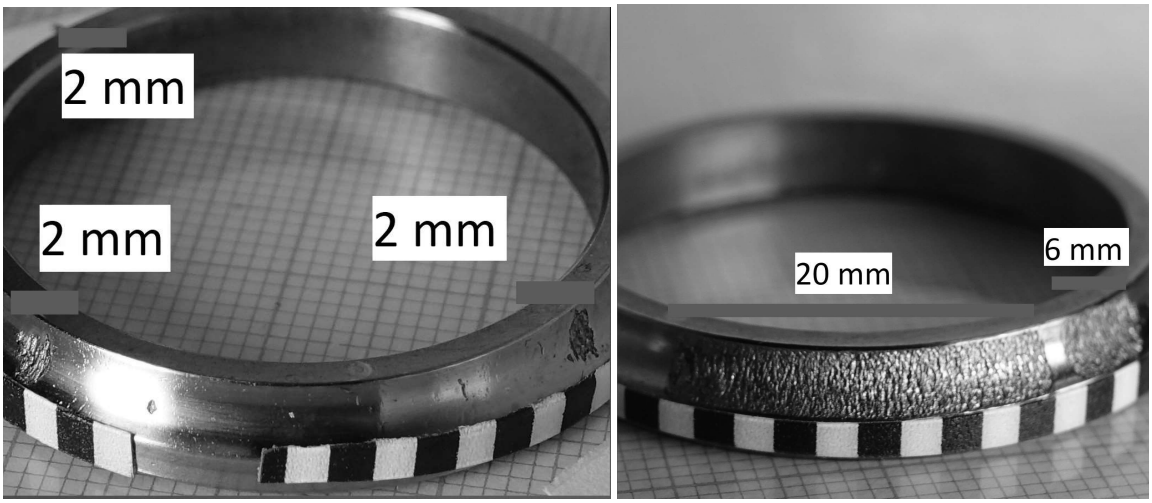

Figure 2: left: DE bearing inner ring after the endurance; right: NDE bearing inner ring after the endurance.

Figure 3: defective balls of the NDE bearing (among a total of five defective balls)

where $y_s(\theta)$ is the averaged signal in angular domain according to the cycle Θ_s of a shaft s.

Note that the high sensitivty of the encoder imposes to substract the deterministic components of all the shafts and gears mesh frequencies of the shaft line, even those physically far from the sensor. This is achieved by projecting the signal $x(\theta)$ in the reference frame of each respective shaft.

Figure 4 (a) presents the evolution of the two bearings' health status during the endurance period. For this purpose, BeaFEM is applied to the cleaned signals. Only the inner ring defect is investigated, by scanning two harmonics and one sideband each time ($H = 2, M = 1$, and $\xi_o = \xi_i = \xi_c = 1$).

Two distinct harmonic sets are visible: the first one is quite energetic, starts at a contact angle $\alpha \simeq 27.5°$ and ends at $\alpha \simeq 34.5°$. The second harmonic set is less energetic than the first one at the end of the experiment; yet it presents a clear amplitude and contact angle evolution. The independent behavior of these two sets suggests that each of them corresponds to the signature of a defect on a distinct bearing.

The coexistence of these harmonic sets has an effect on the indicators presented on figures 4 (b-c)), which were initially designed under the assumption that only one defect was present. Here, the most energetic set is not the same before and after 40 hours of endurance. During the first endurance hours, $I(\alpha_{opt} \simeq 29°)$ is the global maximum while $I(\alpha_{opt} \simeq 28°)$ is only a local maximum. Beyond 40 endurance hours, the greyscale colormap (Figure 4 (a)) highlights a progressive rise of this harmonic set, synonymous with the appearance and propagation of a defect on one of the bearings. The amplitude of the corresponding harmonic set exceeds the other one's and a small jump in the optimal contact angle can be viewed on the figure 4 (b)).

The amplitude elevation indicates a bearing defect evolution, confirmed by the contact angle monotonous elevation (Figure 4 (b)). This last one quickly shifts in the last 38 hours from 29° to 35° which might give indications on the rapid defect evolution. In the background, the other harmonic set starts to increase significantly after 59 hours. This raise is hidden on Figure 4 (b) (c) by the first defect, underlying the importance of the three plots in the analysis process: it clearly indicates the presence of another defect on a bearing whose characteristic frequency is slightly different from the other one.

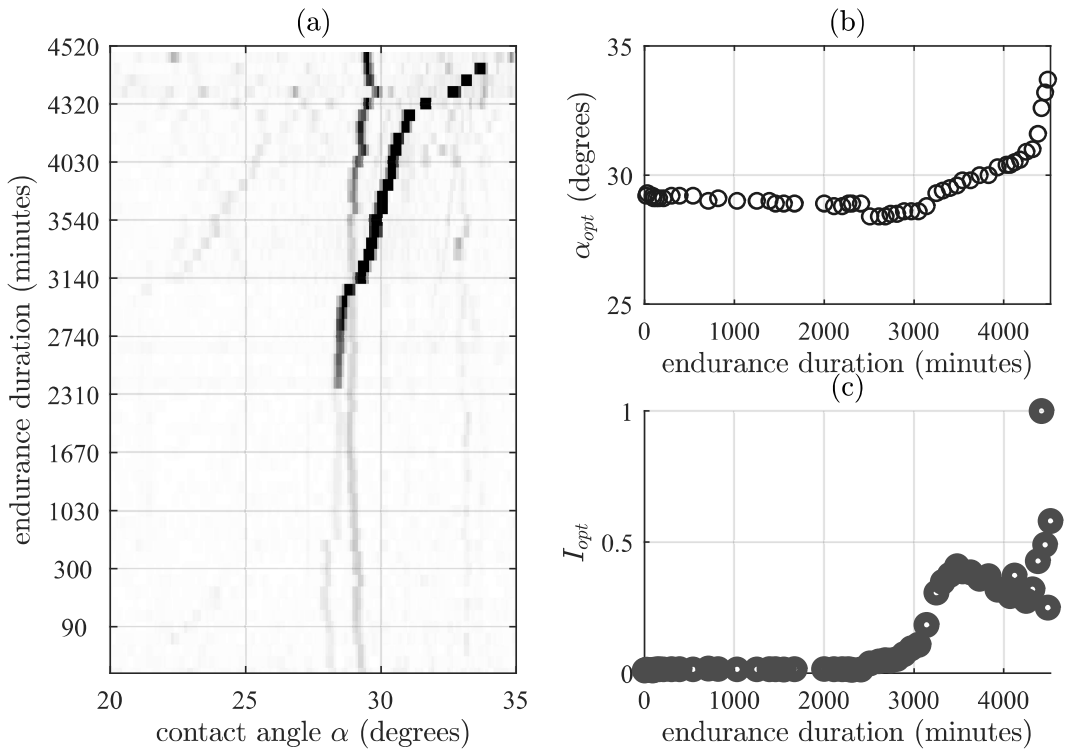

Figure 4: search for inner ring fault during the endurance.(a) $I(\alpha) = f(\alpha, time)$. (b) α_{opt} evolution during the endurance. (c) I_{opt} evolution during the endurance;

4.4 Ball fault search

Figure 5 displays the search for the optimal BSF on the IAS amplitude spectra ($H = 1, M = 0$). Note that the signals are first cleaned in the same way as for the search for the inner ring defect. However, although the representation is identical to facilitate the reading of the results, the method used here does not include one of the keys of the BeaFEM method, and this for two similar reasons:

1. the ball spin characterisitic frequency is expected to experience slippage and shall not stay homokinetic with the other bearing characteristic frequencies. The optimized indicator takes into acount only the harmonic family of the ball defect.

2. since there is no longer a bijection on which to correlate the characteristic frequencies, the optimized argument is no longer alpha but f_{BSF} only.

Considering that the theoretical value is $f_{BSF} = 2.80[epr]$, the result is not very conclusive, since no clear trend emerges. This observation corroborates the statement in section 3 that the ball defect is not visible on the amplitude spectrum since there is no reason for the phenomenon to be CS1. This is because the IAS signal is sampled angularly with respect to the shaft, and the faulty balls slide with respect to this reference.

It is therefore proposed to carry out a CS2 type processing on the IAS signal by analysing the envelope spectrum of the analytic signal filtered between $[10 : 70]epr$ (figure 6). This band of cyclic frequencies chosen by successive iterations makes it possible to bring out the BSF close to its theoretical value ($2.8epr$, visible on figure 6).

BeaFEM application to these signals (figure 7 (a)) indicates the emergence of the BSF around order 2.78. Two lines are actually present, with an uncorrelated time evolution. As endurance increases, the BSF value decreases, indicating an evolution of the system.

At this stage, it is difficult to decide on the cause of this evolution. It may come from the propagation of the defect on the balls, from the generation of defects on new balls, or it may be a consequence of the propagation of the inner ring defect. It should be remembered, however, that only the fundamental frequency of the BSF is monitored in this figure, and that it is therefore its behaviour that is being examined. This observation is supported by the rather monotonous evolution of f_{opt} (figure 7 (b)), particularly after 2200 minutes of testing. Analysing the evolution of I_{opt} is more delicate, but an overall rise in the level is visible from 2500 minutes onwards.

In the end, the application of BeaFEM to a CS2 signal representative of the signature of a ball defect makes it possible to follow the evolution of the latter over time.

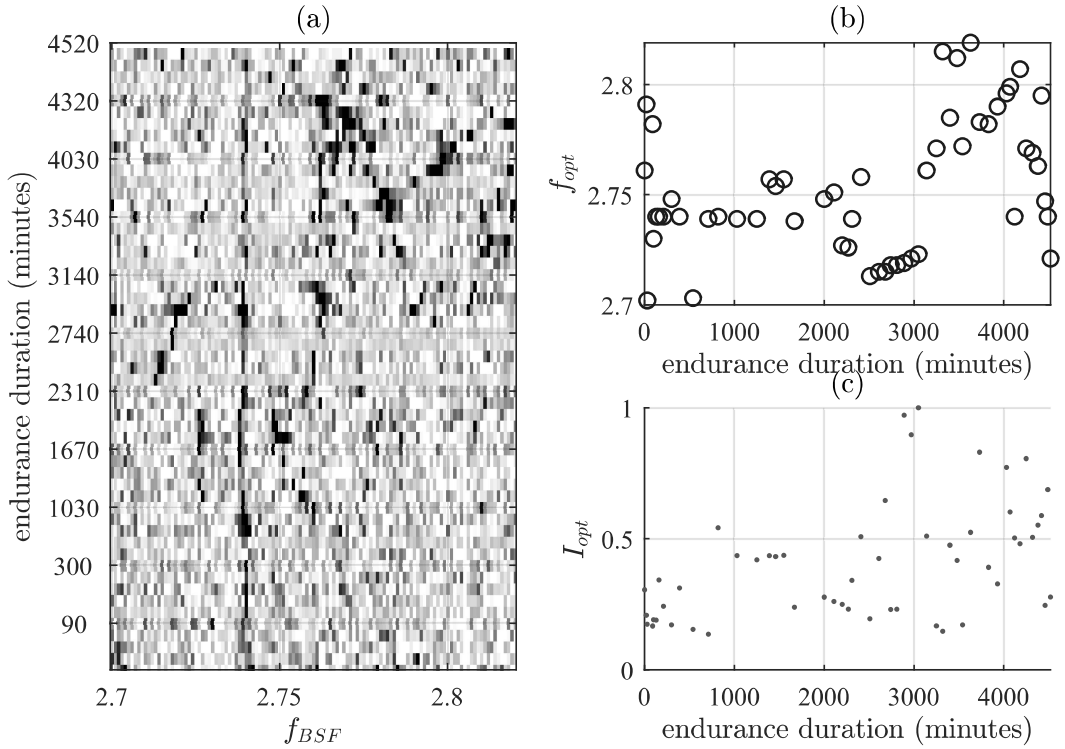

Figure 5: search for ball faults during the endurance; raw signals (corrected).(a) $I(BSF) = f(BSF, time)$. (b) f_{opt} evolution during the endurance. (c) I_{opt} evolution during the endurance;

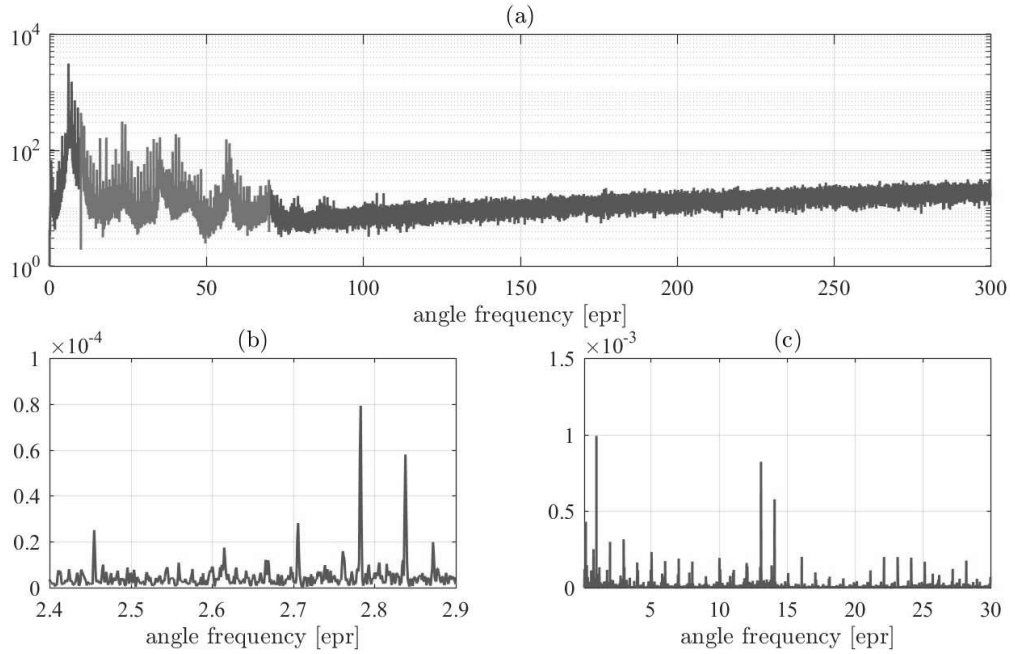

Figure 6: Envelope frequency range.(a) Amplitude Spectrum (raw spectrum; selected band) (b) Squared Envelope Spectrum zoomed on the BSF (c) squared envelope Spectrum

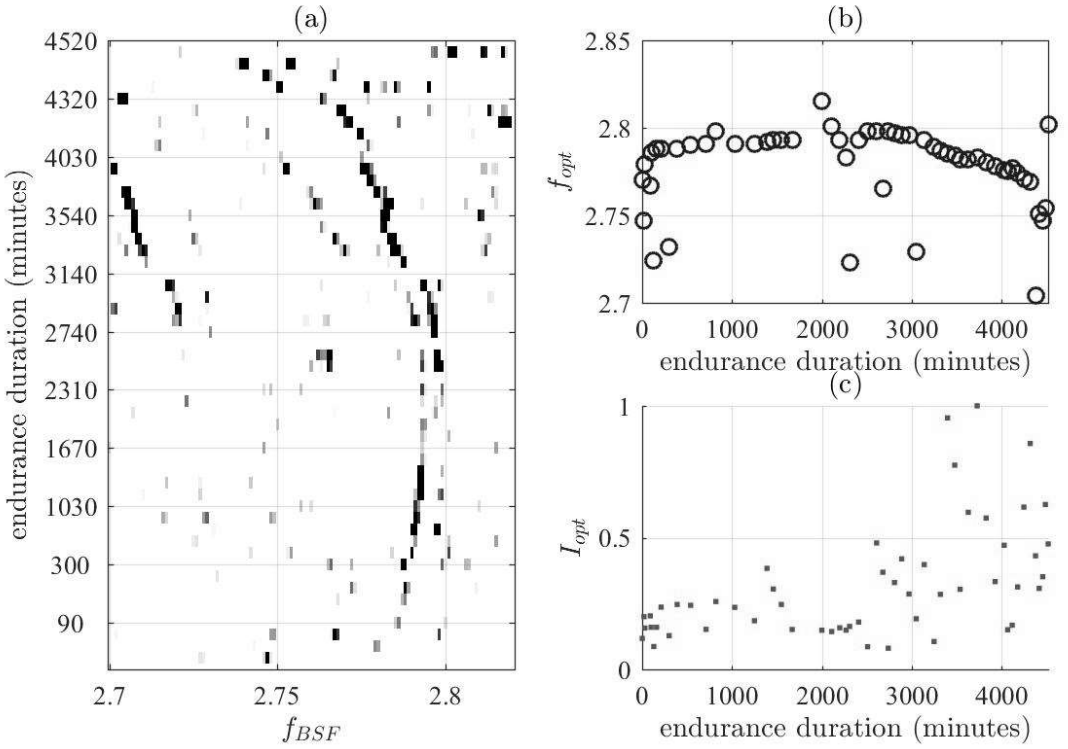

Figure 7: search for ball faults during the endurance; enveloppe signals (corrected, 10-70 epr).(a) $I(BSF) = f(BSF, time)$. (b) f_{opt} evolution during the endurance. (c) I_{opt} evolution during the endurance;

5 Discussion

The implementation of BeaFEM on a first industrial case is promising. Indeed, the test bench used is representative of the industrial scale in terms of operability and measurement environment (background noise, thermal aspects, etc.), and the ageing of the bearings is natural, without strong indentations or artificial defects. The ability to detect a fault in this context is therefore very close to what it would be in a real industrial study.

BeaFEM has several major advantages. Firstly, the pre-processing of the signals by cleaning the kinematic components (unbalance, misalignment, gear mesh frequencies, etc.) is simple, and its effectiveness is facilitated by the angular sampling of the signals: smearing phenomena are avoided. this cleaning is essential for the proper functioning of the algorithm, in order to avoid spurious lines that could be wrongly attributed to defects.

Secondly, the excellent frequency discretization provided by the IAS signals allows a clear observation of the fault formation and of its evolution with a simple pair of scalars: frequency and amplitude of all the bearing characteristic frequencies (BSF appart). The joint study of the indicator level and the optimal angle provides information on the robustness of the detection. The analysis of the spectrogram is nevertheless important: it allows, for example, the identification of the propagation of a second defect of lower amplitude than the main defect.

It should be noted that the way BeaFEM is constructed offers the possibility to discriminate BPFI/BPFO/FTF defects without ambiguity, but requires knowledge of the geometrical characteristics of the bearing.

Initially developed to be applied to CS1 instantaneous rotation speed signals, BeaFEM is also adaptable to CS2 (envelope) signals, thus making it possible to scrutinise the characteristic frequencies of ball defects made so particular by skidding phenomena. this last point is however still at the exploratory stage.

6 Conclusion

This paper proposes a new methodology, BeaFEM, to detect early appearance of bearing faults, and monitor it. In the case of ring or cage defects, the intrinsic angular character of the speed measurement using an encoder allows the use of a basic CS1 approach (i.e. amplitude spectrum), which provides excellent results. Due to the skidding phenomena inherent to bearings, the rolling element fault cannot be analysed using these CS1 tools. It is however possible to adopt a CS2 approach by working on the envelope spectra of the encoder signal. This latter approach is promising for the extension of BeaFEM to classical accelerometer signals. Finally, the excellent sensitivity of IAS signals from encoders leads to the application of the method to signals from sensors located on a shaft not carrying the fault.

7 Acknowledgement

This work was sponsored by the French Direction Générale de l'Armement in the frame of MACCHELI project in partnership with SAFRAN Helicopter Engines.

References

[1] D. E. Butler, "The Shock-pulse method for the detection of damaged rolling bearings," *Non-Destructive Testing*, vol. 6, no. 2, pp. 92–95, 12 1973.

[2] P. D. McFadden and J. D. Smith, "Model for the vibration produced by a single point defect in a rolling element bearing," *Journal of Sound and Vibration*, vol. 96, no. 1, pp. 69–82, 9 1984.

[3] J. Antoni, “Cyclostationarity by examples,” *Mechanical Systems and Signal Processing*, vol. 23, no. 4, pp. 987–1036, 5 2009.

[4] D. Abboud and J. Antoni, “Order-frequency analysis of machine signals,” *Mechanical Systems and Signal Processing*, vol. 87, pp. 229–258, 3 2017. [Online]. Available: http://www.sciencedirect.com/science/article/pii/S0888327016304368?_rdoc=1&_fmt=high&_origin=gateway&_docanchor=&md5=b8429449ccfc9c30159a5f9aeaa92ffb&dgcid=raven_sd_recommender_email

[5] D. Rémond, “Practical performances of high-speed measurement of gear Transmission Error or torsional vibrations with optical encoders,” *Measurement Science and Technology*, vol. 9, no. 3, 1998. [Online]. Available: https://hal.archives-ouvertes.fr/hal-00692560

[6] L. Renaudin, F. Bonnardot, O. Musy, J. B. Doray, and D. Rémond, “Natural roller bearing fault detection by angular measurement of true instantaneous angular speed,” in *Mechanical Systems and Signal Processing*, vol. 24, no. 7. Academic Press, 2010, pp. 1998–2011.

[7] H. André, I. Khelf, and Q. Ere, “Harmonic Product Spectrum revisited and adapted for rotating machine monitoring based on IAS,” *Surveillance*, no. 9, 2017.

[8] J. Antoni and P. Borghesani, “A statistical methodology for the design of condition indicators,” *Mechanical Systems and Signal Processing*, vol. 114, pp. 290–327, 1 2019.

[9] H. André, F. Girardin, and A. Bourdon, “Precision of the IAS monitoring system based on the elapsed time method in the spectral domain,” *Mechanical Systems and Signal Processing*, vol. 44, no. 1-2, pp. 14–30, 2 2014. [Online]. Available: https://www.sciencedirect.com/science/article/pii/S0888327013003038

[10] S. M. Kay and S. L. Marple, “Spectrum analysis—A modern perspective,” *Proceedings of the IEEE*, vol. 69, no. 11, pp. 1380–1419, 1981.

[11] P. Borghesani, P. Pennacchi, R. B. Randall, N. Sawalhi, and R. Ricci, “Application of cepstrum prewhitening for the diagnosis of bearing faults under variable speed conditions,” *Mechanical Systems and Signal Processing*, vol. 36, no. 2, pp. 370–384, 4 2013.

[12] P. D. McFadden and M. M. Toozhy, “APPLICATION OF SYNCHRONOUS AVERAGING TO VIBRATION MONITORING OF ROLLING ELEMENT BEARINGS,” *Mechanical Systems and Signal Processing*, vol. 14, no. 6, pp. 891–906, 11 2000.